Amino acid templating mechanisms in selection of nucleotides opposite abasic sites by a family A DNA polymerase

Samra Obeid[1], Wolfram Welte[2], Kay Diederichs[2], and Andreas Marx[1]

[1]Department of Chemistry, [2]Department of Biology, and [1,2]Konstanz Research School Chemical Biology,
University of Konstanz,
Universitätsstrasse 10, D 78457 Konstanz, Germany

*Running title: Geometric constrains in abasic site bypass

To whom correspondence should be addressed: Prof. Dr. Andreas Marx, Department of Chemistry and Konstanz Research School Chemical Biology, University of Konstanz, Universitätsstrasse 10, D 78457 Konstanz, Germany, Tel.: +49 7531 885139; Fax: +49 7531 885140; Email: andreas.marx@uni-konstanz.de

Background: Abasic site are the most frequent DNA lesion and are often bypassed by incorporating an adenosine opposite that lesion.

Results: Structures of DNA polymerase in complex with different nucleotides opposite an abasic site.

Conclusion: Interaction of the incoming nucleotide with a single amino acid governs nucleotide selection opposite abasic sites.

Significance: Understanding the bypass of a mutagenic lesion by DNA polymerases.

SUMMARY
Cleavage of the *N*-glycosidic bond that connects the nucleobase to the backbone in DNA leads to abasic sites, the most frequent lesion under physiological conditions. Several DNA polymerases preferentially incorporate an A opposite this lesion, a phenomenon termed 'A-rule'. Accordingly, *KlenTaq*, the large fragment of *Thermus aquaticus* DNA polymerase I, incorporates a nucleotide opposite an abasic with efficiencies of A > G > T > C.
Here we provide structural insights into constrains of the active site during nucleotide selection opposite an abasic site. It appears that these confines govern the nucleotide selection mainly by interaction of the incoming nucleotide with Tyr671. Depending on the nucleobase the nucleotides are differently positioned opposite Tyr671

resulting in different alignments of the functional groups that are required for bond formation. The distances between the α–phosphate and the 3'-primer terminus increases in the order A < G < T, which follows the order of incorporation efficiency. Additionally, a binary *KlenTaq* structure bound to DNA containing an abasic site indicates that binding of the nucleotide triggers a remarkable rearrangement of enzyme and DNA template. The ability to resolve the stacking arrangement might be dependent by the intrinsic properties of the respective nucleotide contributing to nucleotide selection.

Furthermore, we studied the incorporation of a non-natural nucleotide opposite an abasic site. The nucleotide was often used in studying stacking effects in DNA polymerization. Here, no interaction with Tyr761 as found for the natural nucleotides is observed indicating a different reaction path for this non-natural nucleotide.

The most common DNA damage under physiological conditions are abasic sites resulting from spontaneous hydrolysis of the *N*-glycosidic bond between the sugar moiety and the nucleobase in DNA (1). Since the genetic information is lost by the cleavage of the nucleobase, abasic sites bear a high mutagenic potential (2-4). In most cases, the lesion is removed by DNA repair systems using the sister strand to guide for incorporation of the right nucleotide. However, undetected lesions or

those, formed during S phase, pose a challenge to DNA polymerases and block replication (5,6). Several studies indicated the mutagenic potential of these lesions in translesion synthesis which is more pronounced in animal compared to bacterial cells presumably due to higher translesion synthesis in eukaryotes (4,7,8) Interestingly, it has been shown that in human cells an adenosine (A) is preferentially incorporated opposite abasic sites (4). Further *in vitro* and *in vivo* studies of DNA polymerases from family A (including human DNA polymerases γ and θ) and B (including human DNA polymerases α, ε and δ) in the presence of the stabilized tetrahydrofuran abasic site analog F (Fig. S1) have shown that purines, in particular adenosine, and to a lesser extent guanosine, are most frequently incorporated opposite the lesion. The strong preference for adenosine has been termed 'A-rule' (7-20).

A set of studies concerning the behavior of DNA polymerases from different sequence families showed that there are multiple mechanisms to overcome an abasic site. Most translesion DNA polymerases follow various loop-out mechanisms (11,21-25). Thereby, the nucleotide selection is influenced by the following upstream templating bases resulting in deletions and complex mutation spectra. Recently, an amino acid templating mechanism was found for the "error-free" bypass of an abasic site by the yeast Rev1 DNA polymerase member of family Y (26). Since guanine is cleaved most frequently (2), the preference of Rev1 for dCMP incorporation opposite an abasic site represents the "best-guess".

However, the determinants of the 'A-rule' are still controversially discussed. Structural and functional studies have added significantly to our understanding of the basic mechanisms of translesion synthesis by DNA polymerases (27,28). Superior stacking as well as solvation properties of adenine have been discussed as driving force behind adenine selection (17,29-31). However, previously reported structures of *KlenTaq*, the large fragment of *T. aquaticus (Taq)* DNA polymerase I, which is a member of the sequence family A, suggests that this enzyme follows the 'A-rule' by applying an amino acid templating mechanism (19,20). Thereby, interaction with Tyr671 seems to be the basis of the preference of purines. It facilitates nucleotide incorporation by mimicking a pyrimidine nucleobase directing for purine incorporation opposite abasic sites due to the enhanced

geometric fit to the active site (32,33). The crucial role of this tyrosine in translesion synthesis, that is highly conserved throughout evolution in DNA polymerase family A from bacteria to humans (34), was further probed by analysis of site-directed mutations (19). Interestingly, when the six-membered ring of tyrosine was mutated to the bicyclic indole of tryptophane the 'A-rule' was shifted to a 'C/T-rule' further supporting geometric factors as determinats of nucleotide selection opposite an abasic site.

Still, several aspects remain to be clarified in order to fully understand the mechanism of nucleotide selection opposite an abasic site by DNA polymerases from the family A. These aspects include the overall conformation of the enzyme-DNA complex in the binary state prior to nucleotide binding. Furthermore, the order of nucleotide incorporation efficiency opposite abasic sites by DNA polymerases like *KlenTaq* is A, G, T and C. The mechanistic understanding for this observation is sparse due to the lack of structural data. Here, we report a structure of a binary complex of *KlenTaq* DNA polymerase bound to the primer/template bearing an abasic site lesion. Additionally, we present several ternary structures of *KlenTaq* caught incorporating different nucleotides opposite an abasic site providing insights into the preference order of nucleotide incorporation efficiency opposite this lesion.

EXPERIMENTAL PROCEDURES

Protein and oligonucleotides. Protein expression and purification was conducted as described (35). In brief, an *E. coli* codon-optimized *KlenTaq* gene (amino acids 293-832 of *Taq* gene; purchased from Geneart, Germany) was cloned into a pET-21b vector without any purification tags and expressed in *E. coli* strain BL21 (DE3). Of note, codon optimization resulted in changes within the gene sequence without affecting the amino acid sequence. After heat denaturation and ultra centrifugation a PEI-precipitation was performed. The resulting material was purified by anion exchange (Q Sepharose) chromatography followed by size-exclusion chromatography (Superdex 75) in 20 mM Tris HCl pH 7.5, 150 mM NaCl, 1 mM EDTA, 1 mM β-mercaptoethanol.

Oligonucleotides were purchased from Metabion (Germany) or Thermo Scientific (Germany). The dideoxy cytosine modified primer was

synthesized on an Applied-Biosystems 392 DNA/RNA synthesizer using the 2',3'-ddC-CPG (5'-dimethoxytrityl-N-succinoyl-long chain alkylamino-CPG, 2',3'-dideoxy cytosine), which was purchased from GLEN RESEARCH, USA. The synthesized oligonucleotide was purified by preparative PAGE on a 12% polyacrylamide gel containing 8 M urea (DMT-OFF). The nucleotide dNITP was synthesized starting from dNI purchased from Berry & Associates Inc., USA, according to published procedures (36).

Crystallization and Structure Determination. *KlenTaq* (buffer: 20 mM Tris HCl pH 7.5, 150 mM NaCl, 1 mM EDTA, 1 mM β-mercaptoethanol) was incubated in presence of DNA primer (5'-d(GAC CAC GGC GC)-3'), an abasic site F containing template (5'-d(AAA FNG CGC CGT GGT C)-3'; N representing the templating base directing for the processing of either ddGTP, ddTTP, or ddCTP.

KlenTaq$_{F-G-I}$: The crystallization was set up using purified *KlenTaq* (11 mg/ml), DNA template/primer duplex, ddGTP in a molar ratio of 1:3:50 and in presence of 20 mM MgCl$_2$. The crystallization solution was mixed in 1:1 ratio with the reservoir solution containing 0.05 M sodium cacodylate (pH 6.5), 0.2 M NH$_4$OAc, 0.01 M Mg(OAc)$_2$, and 25% PEG 8000.

KlenTaq$_{F-G-II}$: As in *KlenTaq*$_{F-G-I}$ using *KlenTaq* (11 mg/ml):DNA template/primer duplex:ddGTP = 1:3:50 in presence of 20 mM MgCl$_2$. The reservoir solution contains 0.05 M sodium cacodylate (pH 6.5), 0.2 M NH$_4$OAc, 0.01 M Mg(OAc)$_2$, and 28% PEG 8000.

KlenTaq$_{F-T}$: As in *KlenTaq*$_{F-G-I}$ using *KlenTaq* (11 mg/ml):DNA template/primer duplex:ddTTP = 1:3:50 in presence of 20 mM MgCl$_2$. The reservoir solution contains 0.05 M sodium cacodylate (pH 6.5), 0.2 M NH$_4$OAc, 0.01 M Mg(OAc)$_2$, and 28% PEG 8000.

KlenTaq$_{F-binary-II}$: As in *KlenTaq*$_{F-G-I}$ using *KlenTaq* (11 mg/ml):DNA template/primer duplex:ddCTP = 1:1.5:60 in presence of 20 mM MgCl$_2$. The reservoir solution contains 0.1 M Tris HCl (pH 8.0), 0.2 M Mg(OAc)$_2$, and 15% PEG 8000.

KlenTaq$_{F-binary}$: The crystallization was set up using purified *KlenTaq* (8 mg/ml), a template (5'-d(AAA FGG CGC CGT GGT C)-3') and a previously synthesized primer with a dideoxy cytosine at its 3'-end, in a molar ratio of 1:1.4 and in presence of 20 mM MgCl$_2$. The crystallization solution was mixed in 1:1 ratio with the reservoir solution containing 0.1 M Tris HCl (pH 7.5), 0.2 M Mg(OAc)$_2$, and 12% PEG 8000.

KlenTaq$_{F-NI}$: As in *KlenTaq*$_{F-binary}$ using *KlenTaq* (8 mg/ml):DNA template/primer duplex = 1:1.4 and in presence of 20 mM MgCl$_2$. The reservoir solution contains 0.1 M Tris HCl (pH 7.0), 0.2 M Mg(OAc)$_2$, and 18% PEG 8000. The crystals were soaked over night by adding 0.5 µl dNITP (20 mM) solution. The occupancy of the bound dNITP was refined to 0.77.

Crystals were produced by the hanging drop vapor diffusion method by equilibrating against 1 ml of the reservoir solution for 5 days at 18°C. The crystals were frozen in liquid nitrogen. Datasets were collected in liquid nitrogen at the beamline PXI (X06SA) at the Swiss Light Source of the Paul Scherrer Institute (PSI) in Villigen, Switzerland, at a wavelength of 1.000/0.900 Å using a PILATUS 6M detector. Data reduction was performed with the XDS package (37,38). The structures were solved by difference Fourier techniques using *KlenTaq* wild type (PDB 3LWL) as model. Refinement was performed with PHENIX (39) and model rebuilding was done with COOT (40). Figures were made with PyMOL (41).

Primer extension assays. Primer extension was performed as described (19). In brief, for incorporation opposite F: 20 µl of the *KlenTaq* reactions contained 100 nM primer (5'-d(CGT TGG TCC TGA AGG AGG ATA GG)-3'), 130 nM template (5'-d(AAA TCA FCC TAT CCT CCT TCA GGA CCA ACG TAC)-3'), 100 µM dNTPs in buffer (20 mM Tris HCl pH 7.5, 50 mM NaCl, and 2 mM MgCl$_2$) and 500 nM of the respective *KlenTaq* polymerase. Reaction mixtures were incubated at 37°C. Incubation times are provided in the respective figure legends. Primer was labelled using [γ-^{32}P]-ATP according to standard techniques. Reactions were stopped by addition of 45 µl stop solution (80% [v/v] formamide, 20 mM EDTA, 0.25% [w/v] bromophenol blue, 0.25% [w/v] xylene cyanol) and analyzed by 12% denaturing PAGE. Visualization was performed by phosphoimaging.

Enzyme kinetics. The rate of single turnovers in pre-steady-state kinetics were determined as described (19). In brief, 15 µl of radiolabelled primer/template complex (200 nM) and DNA polymerase (2 mM) in reaction buffer (see primer extension assay) were rapidly mixed with 15 µl of a dNTP solution in reaction buffer at

37°C. Quenching was achieved by adding previously described stop solution. For reaction times longer than 5 s, a manual quench was performed. The analysis of dNTP incorporation opposite to the abasic site primer (sequences see primer extension assay) and templates (sequences see primer extension assay) were applied. Quenched samples were analyzed on a 12% denaturing PAGE followed by phosphoimaging. For kinetic analysis experimental data were fit by nonlinear regression using the program GraphPad Prism 4. The data were fit to a single exponential equation: [conversion] = A*(1-exp(-k_{obs} t)). The observed catalytic rates (k_{obs}) were then plotted against the dNTP concentrations used and the data were fitted to a hyperbolic equation to determine the K_d of the incoming nucleotide. The incorporation efficiency is given by k_{pol}/K_d.

RESULTS

Overall structure of the KlenTaq complexes in the presence of an abasic site

All *KlenTaq* crystals grew in the same space group and very similar cell parameters (Table S1) as those reported earlier (19,20,35,42-45). Thus, significant differences in crystal packing forces acting on the active site should be negligible. Nevertheless, parts of the finger domain differ in their mobility (as measured by temperature factors) between the different structures. This is a consequence of the structural differences, which were induced in the active site assembly by the primer/template complexes and respective nucleotides that were investigated. In the following, the active sites for the various complexes are shown and described in detail.

Structure of KlenTaq in binary complex with a DNA duplex containing an abasic site (KlenTaq$_{F-binary}$). To address the issue, if the overall conformation of the enzyme-DNA complex is affected by an abasic site prior to nucleotide binding, we crystallized *KlenTaq* bound to primer/template duplex containing an abasic site following a similar strategy as reported recently (19,20,35,43,46). The structure was solved by difference Fourier techniques at a resolution of 1.9 Å (Table S1). *KlenTaq$_{F-binary}$* is very similar to one reported for *KlenTaq* in a binary complex bound to undamaged DNA duplex (PDB 4KTQ; *KlenTaq$_{binary}$*) (35) as reflected by a r.m.s.d. for C$_\alpha$ atoms of 0.60 Å (Fig. 1). However, remarkable structural changes

were observed for the single stranded 5'-overhang of the DNA template, which is rotated around the helical axis. Thereby the lesion is flipped out of a developing DNA duplex (Fig. 1A). This conformation is stabilized by stacking of the 5'-upstream nucleobases of the template strand on the top of the primer/template duplex (Fig. 1B,C) and a distinct hydrogen bonding network of amino acid residues E615 and Y671 with the DNA template (Fig. 1D). In contrast, in *KlenTaq$_{binary}$* the backbone rotates 5' to the DNA duplex redirecting the remainder of the single-stranded template out of the DNA polymerase active site (Fig. 1E).

KlenTaq with ddGTP opposite an abasic site (KlenTaq$_{F-G-I}$, KlenTaq$_{F-G-II}$). To gain insights into the structural basis for the preference of adenosine over guanosine of *KlenTaq* in bypassing an abasic site, we crystallized *KlenTaq* as ternary complex bound to a primer/template duplex and ddGTP opposite the abasic site. Two structures were reproducibly found in several crystallization trials and solved by difference Fourier techniques at resolutions of 2.3 – 2.4 Å (*KlenTaq$_{F-G-I}$* and *KlenTaq$_{F-G-II}$*) (Table S1). The obtained structures show conformational heterogeneity in the active site region. In particular, we found two different orientations of the incoming ddGTP (Fig. 2A,B and Fig. S2A,B). However, the overall conformation of the two ddGTP-trapped structures is very similar to the ternary complex of *KlenTaq* harboring ddATP opposite an abasic site (PDB 3LWL; *KlenTaq$_{F-A}$*; r.m.s.d. for Cα of 0.42 Å) (19), showing the same remarkable structural changes compared to the undamaged case (*KlenTaq* bound to an undamaged primer/template duplex processing a ddGTP; PDB 1QSS; *KlenTaq$_{C-G}$*) (42). Thus, the conformation of the O helix leaves the active site more open similar to the one in *KlenTaq$_{F-A}$* and somehow between the open (PDB 2KTQ; *KlenTaq$_{open}$*) (35) and closed (*KlenTaq$_{C-G}$*) conformations in the reported ternary complexes (Fig. 2E). Like in *KlenTaq$_{F-A}$* we found that the abasic site is intrahelically located and Tyr671 is positioned opposite the incoming ddGTP at the place that is usually occupied by the templating nucleobase (Fig. 2A). However, remarkable differences between *KlenTaq$_{F-A}$* and *KlenTaq$_{F-G-I}$* appear in positioning and interaction pattern of the incoming triphosphates (Fig. 2A and Fig. S3A,B). In *KlenTaq$_{F-G-I}$* Tyr671 stabilizes ddGTP via hydrogen bonds between the Tyr671 hydroxyl group and the N1 of guanine, whereas in *KlenTaq$_{F-A}$* N3 of adenine interacts with

Tyr671 (Fig. 2A and Fig. S3A). Furthermore, an important stabilizing factor of the incoming nucleotide is Arg587. In *KlenTaq*$_{F-A}$ Arg587 forms a hydrogen bond to the N7 of adenine (Fig. S3A). However, in *KlenTaq*$_{F-G-I}$ ddGTP is stabilized by cation-π interaction with Arg587. Since this type of interaction strongly depends on the distribution of the electron density in the aromatic ring system, there is in the case of purines a clear preference for arginine to position itself below or above the imidazole five-atom ring system (47). Indeed, this is observed in *KlenTaq*$_{F-G-I}$ for Arg587 (Fig. 2A,C). The binding arrangement of ddGTP causes a misalignment of the α-phosphate resulting in a large distance of the α-phosphate to the 3'-primer terminus (8.7 Å). Hence, *KlenTaq*$_{F-G-I}$ might represent an initial binding event of the incoming triphosphate (Fig. 2A). In comparison the guanine base in *KlenTaq*$_{F-G-II}$ is rotated around the *N*-glycosidic bond and N7 of guanine points to the hydroxyl group of Tyr671 (Fig. 2B,D and Fig. S2B). Thereby the sugar moiety is realigned resulting in a shortened distance between the α-phosphate and 3'-primer terminus of about 6.9 Å. However, the reorientation of the nucleobase positions the six-membered heterocycle above Arg587 (Fig. 2B,D), a less favored arrangement observed only in rare cases (47). In summary, the distance between 3'-OH and the α-phosphate increases in the following direction *KlenTaq*$_{F-A}$ < *KlenTaq*$_{F-G-II}$ < *KlenTaq*$_{F-G-I}$ that are all longer than the one observed in the canonical case (Fig. 2G).

Pyrimidines opposite an abasic site. Pyrimidine nucleotides are incorporated opposite an abasic site by *KlenTaq* with poor efficiencies (19). Furthermore, we demonstrated that the purine preference could be switched to pyrimidine preference by a single site directed mutagenesis of Tyr671 to Trp (19). This suggests that the low incorporation efficiencies of pyrimidines relies on a specific interactions with this amnio acid residue. To get structural insights we crystallized *KlenTaq* in the presence of a primer/template duplex and ddTTP. The structure was solved by difference Fourier techniques at a resolution of 1.8 Å (*KlenTaq*$_{F-T}$) (Table S1). Although kinetic studies elucidated that thymidine incorporation opposite an abasic site is unfavorable, we observed a bound thymidine triphosphate in the active site (Fig. 3A and Fig. S2C). Once more we obtained a semi-closed enzyme conformation as it can be seen from the superimposition of this structure with *KlenTaq*$_{A-T}$ (PDB 1QTM; processing a canonical

base pair with an incoming ddTTP) (42), *KlenTaq*$_{F-A}$ and *KlenTaq*$_{open}$ (Fig. 3B). The O helix does not pack against the nascent base pair allowing Tyr671 to position itself between the incoming ddTTP and the abasic site as it is observed for Tyr671 in *KlenTaq*$_{F-A}$ (Fig. 3A and Fig. S3A). The ddTTP is stabilized via H-bonding between the N1 of thymidine and the hydroxyl group of Tyr671 as well as π-stacking interactions to Phe667. In contrast to *KlenTaq*$_{F-A}$ in *KlenTaq*$_{F-T}$ Arg587 is released from the stabilization pattern of the incoming triphosphate as it is observed for the purine-trapped stuctures, while still interacting with the phosphate backbone of the 3'-primer terminus. The resulting thymidine tyrosine pair is accommodated in the active site in a way that results in a misalignment of the α-phosphate thereby positions the sugar moiety on top of the 3'-primer terminus (Fig. 3C and 4D).

The same approach as described before was used to co-crystallize *KlenTaq* in the presence of a primer/template duplex and ddCTP (*KlenTaq*$_{F-binary-II}$). However, in all conducted approaches only the formation of binary complexes of *KlenTaq* and the primer/template were obtained. These structures are very similar to the binary structure *KlenTaq*$_{F-binary}$ (Fig. S4).

Nucleotide analog dNITP incorporation opposite an abasic site. Base stacking capability was discussed to play a decisive role in influencing the incorporation efficiency opposite an abasic site (17,31,48-50). Intriguingly, nucleotides that bear nucleobase surrogates with strong stacking but lacking hydrogen bonding capability like 5-nitroindolyl-2'-deoxyriboside 5'-triphosphate (dNITP, Fig. 5A) are incorporated opposite abasic sites with higher efficiency as their natural counterparts. Therefore, non-natural nucleotides like dNITP were used to investigate abasic site bypass as a probe for stacking. To get insights how dNITP is processed opposite an abasic site by *KlenTaq*, we performed soaking experiments with crystals of a binary complex of *KlenTaq* in presence of an abasic site and dNITP. The structure was solved by difference Fourier techniques at a resolution of 1.9 Å (Table S1 and Fig. S2D). In the presence of dNITP the enzyme is accumulated in a closed and productive complex, very similar to reported canonical cases (e.g. PDB 1QTM; *KlenTaq*$_{A-T}$; r.m.s.d. for Cα of 0.53 Å) and in contrast to *KlenTaq*$_{F-A}$ (Fig. 4A,B). In disparity to the structures of *KlenTaq* complexed with natural nucleotides opposite an

abasic site, Tyr671 is released from its stacking interaction to the template strand and provides space for the incoming dNITP (Fig. 4A). The hydrophobic nucleotide analog perfectly stacks on the developing DNA duplex resulting in a proper alignment of the α-phosphate and recruitment of two catalytically essential magnesium ions (Fig. 4C and Fig. S5).

Furthermore, kinetics show that dNIMP is incorporated more efficiently than any other natural nucleotide by *KlenTaq* opposite an abasic site resulting in the following order of incorporation efficiencies (k_{pol}/K_d): NI>>A>G>>T>C (Fig. 5C and Fig. S6A). Due to the decrease in K_d and simultaneous increase in k_{pol}, dNIMP shows a 22-fold increase in incorporation efficiency, compared to dAMP. Interestingly, if *KlenTaq* mutant Y671W is used, we obtained the following incorporation efficiency (k_{pol}/K_d) order NI>C>T>>A>G (Fig. 5D and Fig. S6B). Therefore, one can assume that Tyr671 does not influence the incorporation of dNIMP, whereas it clearly directs the incorporation of the natural nucleotides.

DISCUSSION

General aspects. Although the bypass of a non-instructive lesion by DNA polymerases is extensively studied, the mechanisms are not fully understood yet. Besides starting and end point of chemical reactions non-covalent intermediates with energetic minima are crucial for the reaction pathway. These intermediates are believed to be responsible for pre-selection of nucleotides and represent kinetic checkpoints explaining the overall accuracy and fidelity of these enzymes (51-53). The present structural study provides further insights into how *KlenTaq* DNA polymerase, a member of sequence family A DNA polymerases, is able to bypass abasic sites (Table 1). Independent of the incoming natural nucleotide opposite the abasic site the obtained ternary complexes show two noticeable alterations compared to the canonical cases. Firstly, it is always observed that Tyr671 is placed opposite the incoming nucleotides and secondly, the enzyme adopts a semi-closed conformation. Such a conformation was also associated with mismatch incorporation (54). However, FRET studies of Klenow fragment DNA polymerase in the presence of mismatches indicate that along with the open form the closed state is also partially occupied (55). Since crystallographic data only provides single snapshots, it is likely that in solution there is also a distribution of the populations between the open and closed state even in the presence of an abasic site. Similarly to nucleotide discrimination between matched and mismatched nucleotides, DNA polymerases might also undergo several conformational changes as pre-selection steps before preceding the phosphoryl transfer in the presence of an abasic site. Therefore, the observed conformations might represent various local energy minima along the reaction coordinate. Along these lines, computer simulation of the fidelity of T7 DNA polymerase support the hypothesis that the formation of mismatches may also occur with a high energy barriers from a partially open protein conformation (56). In general, there is an ongoing discussion whether the chemical step demands similar conformational states processing a correct or incorrect nucleotide (52,53,57,58). However, the incoming nucleotides opposite an abasic site in the herein depicted structures are not properly aligned for the phosphoryl transfer. This suggests that either a rearrangement to the closed conformation has to occur or that the incorporation step proceeds from the semi-closed conformation after appropriate conformational changes of the nucleotide. Both scenarios support the observed overall poor incorporation efficiencies opposite abasic sites (19).

Structure of a binary complex containing abasic site and KlenTaq. In the binary complex of *KlenTaq* bound to an abasic site we observed the 5'-upstream template strand stacking on the primer/template duplex. Nucleotide binding forces the release of the template strand from its stacking arrangement and triggers a remarkable rearrangement of the bound DNA template rather than a reorganization of the enzyme (Fig. S7). Furthermore, the ability to resolve the stacking arrangement might be dependent by the intrinsic properties of the respective nucleotide like the stacking and solvation ability of the nucleobase. It remains to be elucidated if this arrangement is sequence specific.

Nucleotide selection opposite absic sites of KlenTaq: adenosines versus guanosines. The structural data offer valuable clues how nucleotide selection is performed opposite a non-instructive lesion and moreover support the previous kinetic analysis of abasic site bypass by *KlenTaq* (19). In case of an incoming guanosine

6

we obtained several crystal structures showing the incoming triphosphate in two different orientations. This heterogeneity was not observed in the presence of the other nucleotides. In $KlenTaq_{F-G-I}$ and $KlenTaq_{F-G-II}$ Tyr671 is filling the space of the vacant nucleobase of the abasic site and is located opposite the incoming ddGTP and thereby roughly mimics the geometry of a nascent nucleobase pair. Of note, such a selection of purines mediated by Tyr671 is also observed for $KlenTaq_{F-A}$. However, in $KlenTaq_{F-G-I}$ and $KlenTaq_{F-G-II}$ the interaction with Tyr671 causes misalignment of the α-phosphate resulting in enlarged distances to the 3'-primer terminus (Fig. 2F and Fig. 6A,B). The different steric constraints of the purine structures account for the preference of adenosine over guanosine. In detail, the exocyclic C_2-NH_2 group of guanine prevents the same arrangement of the nucleotide as it was found for adenosine (Table 1). Due to the steric restriction of the active site the assembly of the sterically more demanding guanosine results in an alignment with an enlarged distance between the α-phosphate and the 3'-primer terminus in comparison to adenosine. Interestingly, the complex showing the stronger cation-π interaction between the Arg587 and the five-membered ring ($KlenTaq_{F-G-I}$) results in an arrangement of the ddGTP obviating a possible attack at the α-phosphate. The closer orientation of the nucleotide towards the 3'-primer terminus suggests that the structure of $KlenTaq_{F-G-II}$ forming a less stable cation-π interaction (47) may represent one step ahead on the reaction coordinate in comparison to $KlenTaq_{F-G-I}$. In conclusion, we find that the distance between the α-phosphates and the 3'-primer terminus (see Table 1, 8.7 - 6.9 Å for guanosines versus 5.9 Å for adenosine) correlates well with the measured incorporation efficiencies. This indicates that active misalignment of the incoming guanosines governs their unfavorable processing by $KlenTaq$ in comparison to adenosines.

Nucleotide selection opposite absic sites by KlenTaq: purines versus pyrimidines. To shine light on the incorporation mechanisms of the less-favored pyrimidines we investigated a structure bearing an incoming ddTTP opposite an abasic site. The DNA polymerase interacts with the incoming nucleotide by hydrogen bonding of Tyr671 with the nucleobase. This results in a nucleoside triphosphate conformation where the sugar moiety is positioned above the 3'-primer terminus instead of the α-phosphate (Fig. 3C and Fig. 6D). In this scenario all components of the active site are assembled and organized in a topological and geometrical arrangement that does not allow the enzyme to proceed with the chemical step explaining the very low incorporation efficiency. In contrast to purines, ddTTP shows low B-factors (Table S1), which indicates that it is well stabilized opposite Tyr671. Thus, the tightly bound thymidine probably stalls the DNA polymerase in a "non-productive" complex by active misalignment, whereas the purine nucleobases enhance the geometric fit to the active site resulting in an arrangement with shortened distances between the α-phosphate and the 3'-primer terminus compared to the pyrimidine base (Fig. 2G and Fig. 6B,E).

Nucleobase stacking and abasic site bypass. Superior stacking and solvation properties of adenine have been discussed as driving force behind adenine selection opposite abasic sites (17,29-31). The nucleotide dNITP contains a nucleobase surrogate lacking hydrogen bonding capability but increased stacking ability in comparison to their structural congener purines. These properties build the basis for the motivation to employ the nucleotide in abasic site bypass (17,31,48-50). We find, in contrast to the results obtained with nucleotides containing the natural nucleobases, that binding of the nucleotide analog dNITP readily allows the enzyme to change its active site conformation in a closed, productive complex that is similar to those found for undamaged DNA substrates. The accumulation of the enzyme in a productive conformation is clearly supported by the kinetic data, which show a significant increase in incorporation efficiency of dNIMP compared to dAMP opposite the abasic site. Furthermore, the circumstance that dNITP is processed with higher efficiency than the favored nucleotides of either $KlenTaq$ wild-type or $KlenTaq$ mutant Y671W shows that Tyr671 apparently lost its selection criteria since both, the dNITP and Tyr671 residues are not compatible with the geometric constrains of the active site. Our results suggest that, due to its increased stacking ability, the nucleobase surrogate imposes active site conformations that differ significantly from those induced by the natural nucleobases. Consequently, results that are obtained by usage of dNITP instead of the natural nucleotides should be interpreted with caution towards their significance in abasic site bypass by natural nucleotides. Noteworthy, dNITP is known as chain terminator (59,60) as

well as universal base (61) and has shown no preference for incorporation opposite one of the four natural nucleobases. Again, enforcement of aberrant enzyme and DNA conformations due to the strong stacking ability of dNITP might be the origin of the observed properties.

Taking together, the present structural study of *KlenTaq* in complex with different nucleoside triphosphates opposite an abasic site reveals that natural nucleotides are bound, due to interaction with Tyr671 and the geometric confines of the active site, in positions that require additional conformational changes for proper alignment in order to facilitate the chemical step. The degree of misalignment, measured as distance of the α-phosphate to the 3'-primer terminus, parallels the order of incorporation efficiency of *KlenTaq* opposite an abasic site. These conformational changes might be accompanied by barriers of varied energy explaining the observed decline in nucleotide incorporation efficiency from A and G to T and C as well as the strong block of the abasic site lesion. The resulting pausing of DNA synthesis might allow the DNA polymerase to be replaced by repair systems that use the sister strand for error-free repair.

The human DNA polymerase θ and γ are members of the sequence family A as *KlenTaq*. Interestingly, the human DNA polymerase θ also obeys the 'A-rule' (18) and its intrinsically error-prone abasic-site bypass might contribute in somatic hypermutation of Ig genes (62). Furthermore, the role of Tyr671 in nucleotide selection opposite an abasic site is highlighted. Tyr671 is highly conserved in family A DNA polymerases (19,34) and is known to be involved in the discrimination process between canonical and non-canonical base pairs (63-65). Along these lines, Leob and coworkers demonstrated that Tyr671 is essential for maintaining *Taq* DNA polymerase I activity (63). Mutations at that position are hardly tolerated and compromise activity with the exception of phenylalanine. Nevertheless, mutations of the homolog residue Tyr766 of the Klenow fragment from *E. coli* DNA polymerase I to serine or alanine result in significant decrease in fidelity (64). Interestingly, mutation of the corresponding Tyr955 in human DNA polymerase γ has been attributed to progressive external ophthalmoplegia (PEO) stressing its importance in accurate function of DNA polymerases (66,67).

REFERENCES

1. Lindahl, T. (1993) *Nature* **362**, 709-715
2. Preston, B. (1986) *Annu. Rev. Genet.* **20**, 201-230
3. Hoeijmakers, J. H. (2001) *Nature* **411**, 366-374
4. Avkin, S., Adar, S., Blander, G., and Livneh, Z. (2002) *Proc. Natl. Acad. Sci. U. S. A.* **99**, 3764-3769
5. Goodman, M. F., Cai, H., Bloom, L. B., and Eritja, R. (1994) *Ann. N. Y. Acad. Sci.* **726**, 132-142
6. Hubscher, U., Maga, G., and Spadari, S. (2002) *Annu. Rev. Biochem.* **71**, 133-163
7. Pagès, V., Johnson, R. E., Prakash, L., and Prakash, S. (2008) *Proc. Natl. Acad. Sci. U. S. A.* **105**, 1170-1175
8. Schaaper, R. M., Kunkel, T. A., and Loeb, L. A. (1983) *Proc. Natl. Acad. Sci. U. S. A.* **80**, 487-491
9. Sagher, D., and Strauss, B. (1983) *Biochemistry* **22**, 4518-4526
10. Randall, S. K., Eritja, R., Kaplan, B. E., Petruska, J., and Goodman, M. F. (1987) *J. Biol. Chem.* **262**, 6864-6870
11. Efrati, E., Tocco, G., Eritja, R., Wilson, S. H., and Goodman, M. F. (1997) *J. Biol. Chem.* **272**, 2559-2569
12. Shibutani, S., Takeshita, M., and Grollman, A. P. (1997) *J. Biol. Chem.* **272**, 13916-13922
13. Strauss, B. S. (2002) *DNA Repair* **1**, 125-135
14. Taylor, J.-S. (2002) *Mutat. Res.* **510**, 55-70
15. Freisinger, E., Grollman, A. P., Miller, H., and Kisker, C. (2004) *EMBO J.* **23**, 1494-1505
16. Hogg, M., Wallace, S. S., and Doublié, S. (2004) *EMBO J.* **23**, 1483-1493
17. Reineks, E. Z., and Berdis, A. J. (2004) *Biochemistry* **43**, 393-404
18. Seki, M., Masutani, C., Yang, L. W., Schuffert, A., Iwai, S., Bahar, I., and Wood, R. D. (2004) *EMBO J.* **23**, 4484-4494

19. Obeid, S., Blatter, N., Kranaster, R., Schnur, A., Diederichs, K., Welte, W., and Marx, A. (2010) *EMBO J.* **29**, 1738-1747

20. Obeid, S., Schnur, A., Gloeckner, C., Blatter, N., Welte, W., Diederichs, K., and Marx, A. (2011) *ChemBioChem* **12**, 1574-1580

21. Ling, H., Boudsocq, F., Woodgate, R., and Yang, W. (2004) *Mol. Cell* **13**, 751-762

22. Fiala, K. A., Hypes, C. D., and Suo, Z. (2007) *J. Biol. Chem.* **282**, 8188-8198

23. Nair, D. T., Johnson, R. E., Prakash, L., Prakash, S., and Aggarwal, A. K. (2009) *Structure (London)* **17**, 530-537

24. Choi, J.-Y., Lim, S., Kim, E.-J., Jo, A., and Guengerich, F. P. (2010) *J. Mol. Biol.* **404**, 34-44

25. Sherrer, S. M., Fiala, K. A., Fowler, J. D., Newmister, S. A., Pryor, J. M., and Suo, Z. (2011) *Nucleic Acids Res.* **39**, 609-622

26. Nair, D. T., Johnson, R. E., Prakash, L., Prakash, S., and Aggarwal, A. K. (2011) *J. Mol. Biol.* **406**, 18-28

27. Yang, W., and Woodgate, R. (2007) *Proc. Natl. Acad. Sci. U. S. A.* **104**, 15591-15598

28. Zahn, K. E., Wallace, S. S., and Doublie, S. (2011) *Curr Opin Struct Biol* **21**, 358-369

29. Matray, T. J., and Kool, E. T. (1999) *Nature* **399**, 704-708

30. Hwang, H., and Taylor, J.-S. (2004) *Biochemistry* **43**, 14612-14623

31. Zahn, K. E., Belrhali, H., Wallace, S. S., and Doublié, S. (2007) *Biochemistry* **46**, 10551-10561

32. Goodman, M. F. (1997) *Proc. Natl. Acad. Sci. U. S. A.* **94**, 10493-10495

33. Kool, E. T. (2002) *Annu. Rev. Biochem.* **71**, 191-219

34. Delarue, M., Poch, O., Tordo, N., Moras, D., and Argos, P. (1990) *Protein Eng.* **3**, 461-467

35. Li, Y., Korolev, S., and Waksman, G. (1998) *EMBO J.* **17**, 7514-7525

36. Di Pasquale, F., Fischer, D., Grohmann, D., Restle, T., Geyer, A., and Marx, A. (2008) *J. Am. Chem. Soc.* **130**, 10748-10757

37. Kabsch, W. (2010) *Acta Crystallogr. D* **66**, 125-132

38. Kabsch, W. (2010) *Acta Crystallogr. D* **66**, 133-144

39. Adams, P. D., Grosse-Kunstleve, R. W., Hung, L. W., Ioerger, T. R., McCoy, A. J., Moriarty, N. W., Read, R. J., Sacchettini, J. C., Sauter, N. K., and Terwilliger, T. C. (2002) *Acta Crystallogr. D* **58**, 1948-1954

40. Emsley, P., and Cowtan, K. (2004) *Acta Crystallogr. D* **60**, 2126-2132

41. DeLano, W. (2002) *The PyMOL Molecular Graphics System*, DeLano Scientific, Palo Alto, CA

42. Li, Y., Mitaxov, V., and Waksman, G. (1999) *Proc. Natl. Acad. Sci. U. S. A.* **96**, 9491-9496

43. Li, Y., and Waksman, G. (2001) *Protein Sci.* **10**, 1225-1233

44. Obeid, S., Baccaro, A., Welte, W., Diederichs, K., and Marx, A. (2010) *Proc. Natl. Acad. Sci. U. S. A.* **107**, 21327-21331

45. Betz, K., Streckenbach, F., Schnur, A., Exner, T., Welte, W., Diederichs, K., and Marx, A. (2010) *Angew. Chem., Int. Ed. Engl.* **49**, 5181-5184

46. Korolev, S., Nayal, M., Barnes, W. M., Di Cera, E., and Waksman, G. (1995) *Proc. Natl. Acad. Sci. U. S. A.* **92**, 9264-9268

47. Wintjens, R., Liévin, J., Rooman, M., and Buisine, E. (2000) *J. Mol. Biol.* **302**, 395-410

48. Vineyard, D., Zhang, X., Donnelly, A., Lee, I., and Berdis, A. J. (2007) *Org. Biomol. Chem.* **5**, 3623-3630

49. Sheriff, A., Motea, E., Lee, I., and Berdis, A. J. (2008) *Biochemistry* **47**, 8527-8537

50. Motea, E. A., Lee, I., and Berdis, A. J. (2011) *Nucleic Acids Res.* **39**, 1623-1637

51. Joyce, C. M., and Benkovic, S. J. (2004) *Biochemistry* **43**, 14317-14324

52. Johnson, K. A. (2010) *Biochim. Biophys. Acta, Proteins Proteomics* **1804**, 1041-1048

53. Joyce, C. M. (2010) *Biochim. Biophys. Acta, Proteins Proteomics* **1804**, 1032-1040

54. Wu, E. Y., and Beese, L. S. (2011) *J. Biol. Chem.* **286**, 19758-19767

55. Santoso, Y., Joyce, C. M., Potapova, O., Le Reste, L., Hohlbein, J., Torella, J. P., Grindley, N. D. F., and Kapanidis, A. N. (2010) *Proc. Natl. Acad. Sci. U. S. A.* **107**, 715-720

56. Florián, J., Goodman, M. F., and Warshel, A. (2005) *Proc. Natl. Acad. Sci. U. S. A.* **102**, 6819-6824

57. Batra, V. K., Beard, W. A., Shock, D. D., Pedersen, L. C., and Wilson, S. H. (2008) *Mol. Cell* **30**, 315-324

58. Beese, L. (2011) *J. Biol. Chem.* **286**, 19758-19767
59. Smith, C. L., Simmonds, A. C., Felix, I. R., Hamilton, A. L., Kumar, S., Nampalli, S., Loakes, D., Hill, F., and Brown, D. M. (1998) *Nucleosides, Nucleotides Nucleic Acids* **17**, 541-554
60. Loakes, D. (2001) *Nucleic Acids Res* **29**, 2437-2447
61. Loakes, D., and Brown, D. M. (1994) *Nucleic Acids Res* **22**, 4039-4043
62. Masuda, K., Ouchida, R., Hikida, M., and Kurosaki, T. (2007) *J. Biol. Chem.* **282**, 17387-17394
63. Suzuki, M., Baskin, D., Hood, L., and Loeb, L. A. (1996) *Proc. Natl. Acad. Sci. U. S. A.* **93**, 9670-9675
64. Bell, J. B., Eckert, K. A., Joyce, C. M., and Kunkel, T. A. (1997) *J. Biol. Chem.* **272**, 7345-7351
65. Minnick, D. T., Bebenek, K., Osheroff, W. P., Turner, R. M., Astatke, M., Liu, L., Kunkel, T. A., and Joyce, C. M. (1999) *J. Biol. Chem.* **274**, 3067-3075
66. Copeland, W. C., Ponamarev, M. V., Nguyen, D., Kunkel, T. A., and Longley, M. J. (2003) *Acta Biochim. Pol.* **50**, 155-167
67. Graziewicz, M. A., Longley, M. J., Bienstock, R. J., Zeviani, M., and Copeland, W. C. (2004) *Nat. Struct. Mol. Biol.* **11**, 770-776

FIGURE LEGENDS

FIGURE 1 Structure of *KlenTaq*$_{F-binary}$ (blue). A. Template stacking assembly of A_{n+2} and A_{n+3} in *KlenTaq*$_{F-binary}$. The abasic site analog F_{n+1} is located extrahelically. B. The stick and surface depiction highlights the template stacking arrangement. C. Top view of the primer template sacking arrangement. D. Hydrogen bonding network of the amino acid side chains Y671 and E615 with the template strand. E. Same arrangement as in A. for the superimpositioned structures of *KlenTaq*$_{F-binary}$ (blue) and *KlenTaq*$_{binary}$ (brown).

FIGURE 2 Structure of *KlenTaq*$_{F-G-I}$ (black) and *KlenTaq*$_{F-G-II}$ (gray). A. Stabilization network of ddGTP in *KlenTaq*$_{F-G-I}$. Labelled are the amino acid side chain R587 and Y671. Gray, red and black dashed lines indicate hydrogen-bonding interactions, cation-π interaction and distance (Å), respectively. B. The same as in A. for *KlenTaq*$_{F-G-II}$. C. Top view of the nascent base pair opposite F (*KlenTaq*$_{F-G-I}$). In the front the incoming ddGTP opposite Y671 is depicted. In transparent the first nucleobase pair of the primer template terminus is shown. D. Same view as in C. for *KlenTaq*$_{F-G-II}$. E. Highlighted are the O helices from the superimposition of *KlenTaq*$_{F-G-II}$ (gray), *KlenTaq*$_{F-A}$ (purple), *KlenTaq*$_{C-G}$ (green) and *KlenTaq*$_{open}$ (golden). F. Comparison of the nascent base pairs of *KlenTaq*$_{F-G-II}$ (gray), *KlenTaq*$_{F-A}$ (purple), *KlenTaq*$_{C-G}$ (green). G. Shown are the incoming ddNTPs of *KlenTaq*$_{F-G-II}$ (gray), *KlenTaq*$_{F-A}$ (purple), *KlenTaq*$_{C-G}$ (green) and the respective 3'-primer terminus. Arrow indicates the displacement of the α-phosphate regarding to the 3'-primer terminus.

FIGURE 3 Structure of *KlenTaq*$_{F-T}$ (yellow). A. Stabilization network of ddTTP. Labelled are the amino acid side chain R587, F667 and Y671. Gray and black dashed lines indicate hydrogen-bonding interactions and distance (Å), respectively. B. Highlighted are the O helices from the superimposition of *KlenTaq*$_{F-T}$ (yellow), *KlenTaq*$_{F-A}$ (purple), *KlenTaq*$_{A-T}$ (berry) and *KlenTaq*$_{binary}$ (golden). C. Shown are the incoming ddNTPs of *KlenTaq*$_{F-T}$ (yellow), *KlenTaq*$_{F-A}$ (purple), *KlenTaq*$_{A-T}$ (berry) and the respective 3'-primer terminus. Arrow indicates the displacement of the α-phosphate regarding to the 3'-primer terminus.

FIGURE 4 Structure of *KlenTaq*_{F-NI} (orange). A. Stabilization network of dNITP. Labelled are the amino acid side chain R587, F667 and Y671. Black dashed lines indicate distance (Å). B. Highlighted are the O helices from the superimposition of *KlenTaq*_{F-NI} (cyan), *KlenTaq*_{F-A} (purple), *KlenTaq*_{C-G} (green) and *KlenTaq*_{binary} (golden). C. Shown are the incoming ddNTPs of *KlenTaq*_{F-NI} (cyan) and *KlenTaq*_{C-G} (green), the respective Mg^{2+} ions and the respective catalytically relevant residues D610, Y611 and D785.

FIGURE 5 Nucleotide incorporation opposite an abasic site analog F. A. Structure of nucleotide analog dNITP. B. Partial primer template sequence used in primer extension experiments. C. Single nucleotide incorporation of *KlenTaq* wild type opposite F for 1, 10, or 60 min, respectively. The respective dNTP is indicated. Transient kinetic analysis of nucleotide incorporation opposite T/F by *KlenTaq* wild type. * Kinetic data are first reported in (19). D. Single nucleotide incorporation of *KlenTaq* Y671W mutant opposite F for 10, 60, or 120 min, respectively. The respective dNTP is indicated. Transient kinetic analysis as in C. for *KlenTaq* Y671W.

FIGURE 6 Geometry fit to the active site. A. Active site assembly in the presence of an abasic site analog F. Nascent base pair of Y671 and ddGTP (*KlenTaq*_{F-G-I}) is depicted. The surface of the surrounding active site residues is shown in gray. B. Same as in A. for *KlenTaq*_{F-G-II}. C. Active site assembly in the case of an undamaged template showing the nascent base pair of dC and ddGTP (*KlenTaq*_{C-G}). D. Same as in A. for *KlenTaq*_{F-T}. E. Same as in A. for *KlenTaq*_{F-A}. F. Same as in C. for *KlenTaq*_{F-NI} showing the nascent base pair of F and dNITP. A.-F. The arrows indicate the positioning of the α-phosphate and the 3'-primer terminus, respectively.

Table 1 Summary of *KlenTaq* structures bound to an abasic site analog F

Figure 1

Figure 2

Figure 3

Figure 4

Figure 5

A dNITP

B
5'- ... TAGG
3'- ... ATCC **F** ACT → dNTP

C KTQ wt

N: -   NI   A   G   T   C

time:

24 nt
23 nt

N/F-dNTP	K_d [µM]	k_{pol} [s^{-1} x10^{-2}]	k_{pol}/K_d [$M^{-1}*s^{-1}$ x10^{-4}]
T-dATP*	15.3±4.7	516±44	3373
F-dATP*	149±35	2.73±0.23	1.83
FdNITP	19.7±1.1	7.80±1.12	39.5

D KTQ Y671W

N: -   NI   A   G   T   C

time:

24 nt
23 nt

N/F-dNTP	K_d [µM]	k_{pol} [s^{-1} x10^{-2}]	k_{pol}/K_d [$M^{-1}*s^{-1}$ x10^{-4}]
T-dATP*	363±104	91.6±15.2	25.2
F-dCTP*	845±161	0.92±0.12	0.11
F-dATP*	514±182	0.10±0.02	0.02
FdNITP	97.8±24.4	0.24±0.02	0.25

16
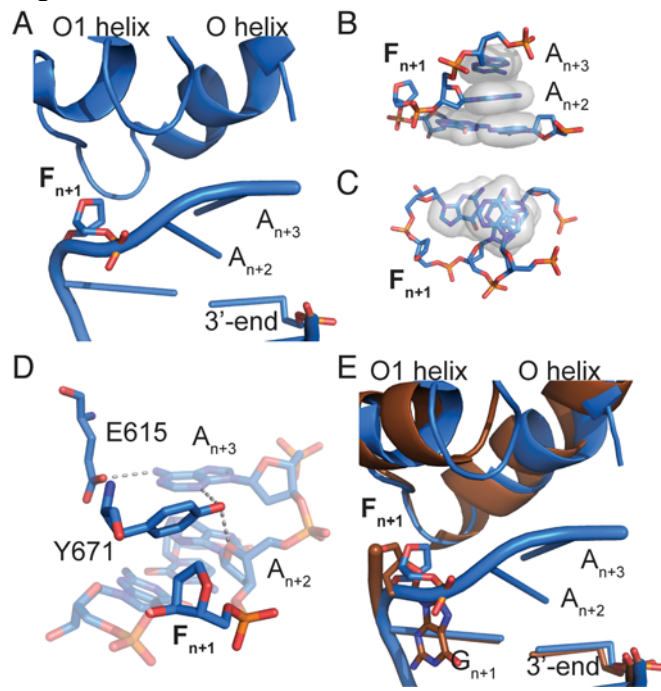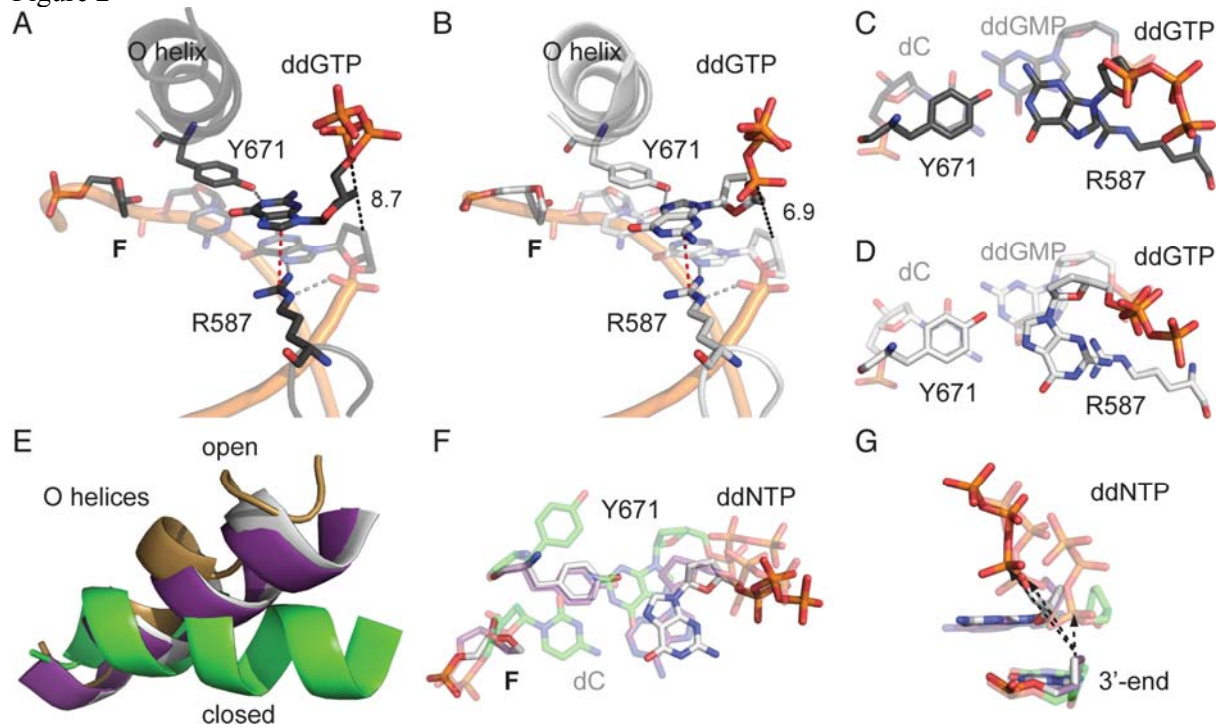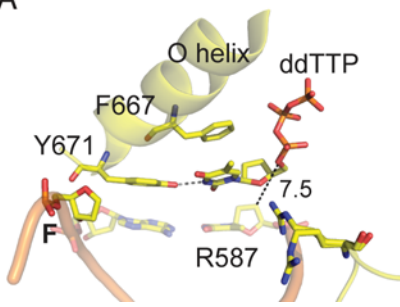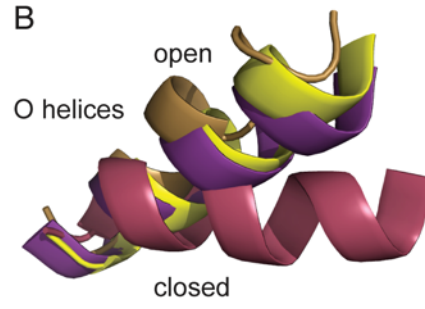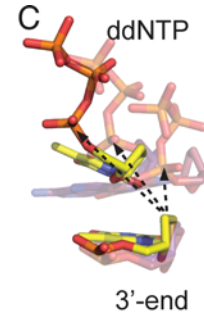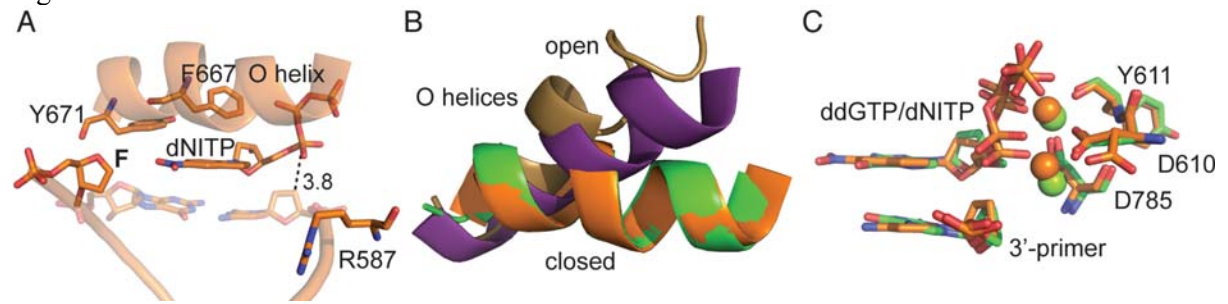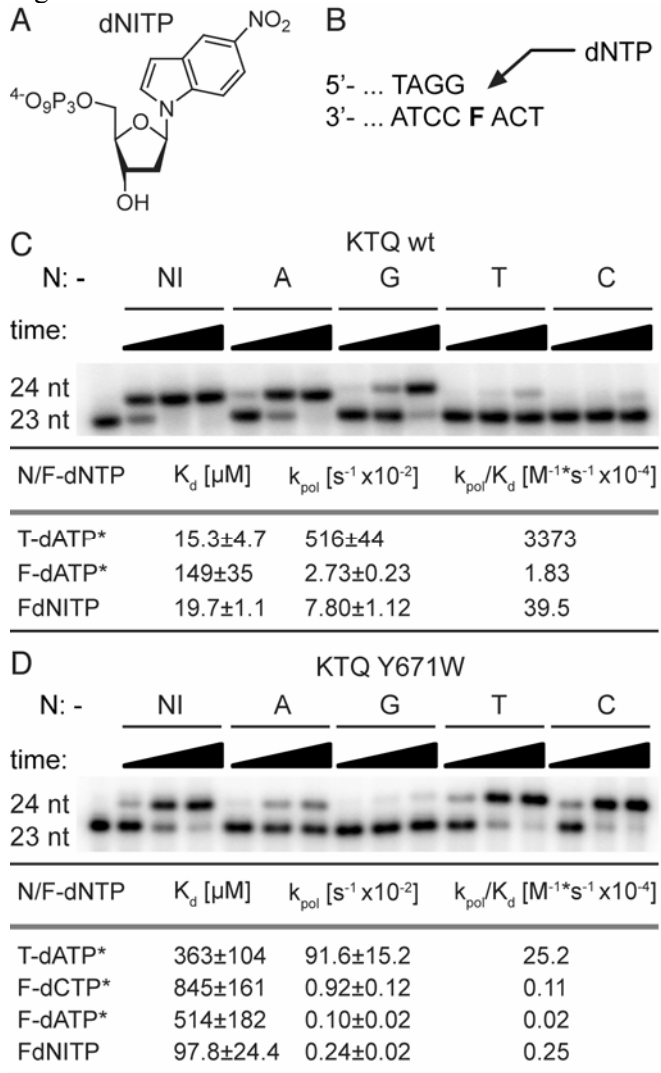
Figure 6
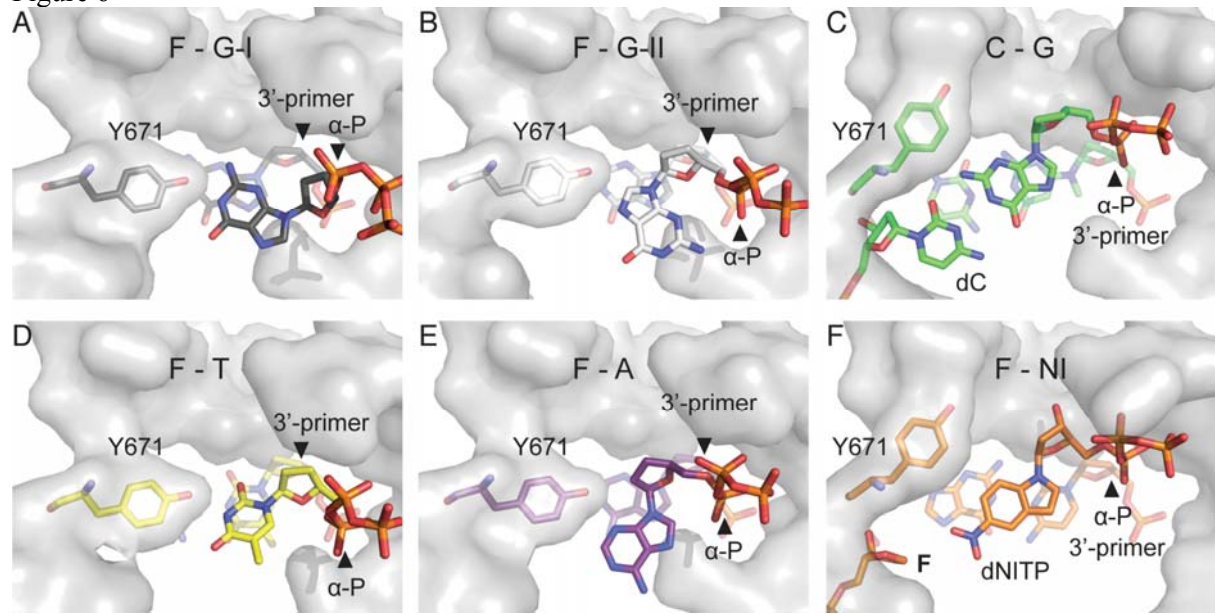
Table 1

F - A	F - G-I	F - G-II	F - T	F - binary	F - NI
Y671 positioned opposite ddATP	Y671 positioned opposite ddGTP	Y671 positioned opposite ddGTP	Y671 positioned opposite ddTTP	Y671 is released from stacking interaction to the template strand	Y671 is released from stacking interaction to the template strand
H-bond N3-ddATP – OH-Y671	H-bond N1-ddGTP – OH-Y671	H-bond N7-ddGTP – OH-Y671	H-bond N1-ddTTP – OH-Y671	--	--
R587 stabilizes the phosphate-backbone of the 3'-primer terminus	R587 stabilizes the phosphate-backbone of the 3'-primer terminus	R587 stabilizes the phosphate-backbone of the 3'-primer terminus	R587 stabilizes the phosphate-backbone of the 3'-primer terminus	R587 stabilizes the phosphate-backbone of the 3'-primer terminus	R587 stabilizes the phosphate-backbone of the 3'-primer terminus
H-bond N7-ddATP – R587	cation-π interaction between 5-cyclic ring and R587	cation-π interaction between 6-cyclic ring and R587	--	--	--
F located intrahelically	F located intrahelically	F located intrahelically	F located intrahelically	F located extrahelically	F located intrahelically
1 Mg^{2+} ion is complexed by ddATP	--	--	1 Mg^{2+} ion is complexed by ddTTP	--	2 Mg^{2+} ion are complexed by ddNITP
P_α – 3'-primer terminus: 5.9 Å	α-P – 3'-primer terminus: 8.7 Å	α-P – 3'-primer terminus: 6.9 Å	α-P – 3'-primer terminus: 7.5 Å	--	α-P – 3'-primer terminus: 7.5 Å
PDB-ID: 3LWL	PDB-ID: 3RR8	PDB-ID: 3RRG	PDB-ID: 3RRH	PDB-ID: 3RR7	PDB-ID: 3T3F